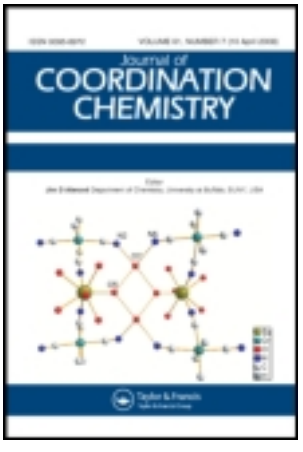

Journal of Coordination Chemistry
Publication details, including instructions for authors and subscription information:
http://www.tandfonline.com/loi/gcoo20

Crystal structures and DNA cleavage activities of two mononuclear nickel(II) complexes

Jie Xu [a], Yun-feng Chen [a], Hong Zhou [a] & Zhi-quan Pan [a]
[a] Key Laboratory for Green Chemical Process of Ministry of Education, Wuhan Institute of Technology, Wuhan 430073, P.R. China
Published online: 04 May 2011.

To cite this article: Jie Xu, Yun-feng Chen, Hong Zhou & Zhi-quan Pan (2011) Crystal structures and DNA cleavage activities of two mononuclear nickel(II) complexes, Journal of Coordination Chemistry, 64:9, 1626-1635, DOI: 10.1080/00958972.2011.563384

To link to this article: http://dx.doi.org/10.1080/00958972.2011.563384

Journal of Coordination Chemistry
Vol. 64, No. 9, 10 May 2011, 1626–1635

Crystal structures and DNA cleavage activities of two mononuclear nickel(II) complexes

JIE XU, YUN-FENG CHEN, HONG ZHOU* and ZHI-QUAN PAN*

Key Laboratory for Green Chemical Process of Ministry of Education,
Wuhan Institute of Technology, Wuhan 430073, P.R. China

(*Received 28 November 2010; in final form 10 January 2011*)

Two new nickel complexes, $[Ni(L_1)_2] \cdot 2(CH_3OH)$ (**1**) and $[Ni(L_2)_2] \cdot 2(CH_3OH)$ (**2**), where HL_1 is 4-chloro-2-((2-hydroxy-ethylimino)methyl)phenol and HL_2 is 4-fluoro-2-((2-hydroxy-ethylimino)methyl)phenol, have been synthesized and characterized by single-crystal X-ray diffraction and UV-Vis absorption spectra. The coordination polyhedron of nickel(II) in each complex can be described as distorted octahedral. The interactions between the complexes and calf thymus (CT)-DNA/DNA were investigated by UV-Vis spectra and agarose gel electrophoresis. The results show that the complex transforms supercoiled to nicked form and exhibits effective DNA cleavage activity *via* hydrolytic cleavage mechanism.

Keywords: Nickel complexes; Crystal structure; DNA cleavage activities

1. Introduction

Hydrolysis of phosphodiester bonds of DNA by nucleases shows that the enormous effects of these enzymes depend on the presence of metal ions in their active sites and noncovalent bonding with DNA [1]. To search for restriction enzymes and anticancer therapeutic agents, much effort has been made in the syntheses and properties of mimics. Some transition metal complexes have exhibited high DNA cleavage activities [2, 3]. These complexes can be bound to DNA in many noncovalent modes, such as ionic bonds, hydrogen bonds, π–π interactions, and hydrophobic interactions. The noncovalent interactions hold the complexes and DNA together, and enable the complexes and DNA binding, and in turn increase the cleavage activity of the complexes. The metal ions and the structures of the ligand in complexes are the key factors for hydrolysis activities of the complexes [4,5].

Complexes derived from 4-X-2-[(2-hydroxy-ethylamino)methyl]phenol (X = Br, NO_2) have been structurally characterized [6–8]. However, the structures of this kind of complexes with X = F and Cl have not been reported. Herein, two mononuclear Ni(II) complexes of 4-X-2-((2-hydroxy-ethylimino)methyl)phenol (X = F and Cl) were synthesized and characterized. The complexes are expected to interact with DNA *via* hydrogen-bonding or π–π interactions because of abundant donor atoms and aromatic

*Corresponding authors. Email: hzhou126@163.com; zhiqpan@163.com

Journal of Coordination Chemistry
ISSN 0095-8972 print/ISSN 1029-0389 online © 2011 Taylor & Francis
DOI: 10.1080/00958972.2011.563384

rings in their structures. These noncovalent interactions might serve to promote DNA cleavage activity and DNA cleavage activities of the two complexes are also investigated.

2. Experimental

2.1. *Preparations*

5-Chlorosalicylaldehyde and 5-fluorosalicylaldehyde were recrystallized from ethanol before use; other chemicals and solvents were of analytical grade and used as received. Calf thymus-DNA (CT-DNA) was obtained from Sigma and used as received.

2.2. *Synthesis of complexes*

2.2.1. $[Ni(L_1)_2] \cdot 2(CH_3OH)$ (1). To a solution of 5-chlorosalicylaldehyde (0.312 g, 2 mmol), $Ni(CH_3COO)_2 \cdot 4H_2O$ (0.248 g, 1 mmol) in absolute methanol (30 mL), and 2-aminoethanol (0.122 g, 2 mmol) in absolute methanol (15 mL) were slowly added, giving a bright green solution. The mixture was stirred at room temperature for 5 h, and then triethylamine (1 mL) was introduced. The resulting solution was stirred at ambient temperature for 24 h, filtered, and the resulting solution was allowed to evaporate slowly. Green block crystals suitable for X-ray measurement were collected. Yield: 0.369 g (71%). Anal. Calcd for $C_{20}H_{26}Cl_2N_2NiO_6$ (%): C, 46.19; H, 5.04; N, 5.39. Found (%): C, 46.33; H, 5.14; N, 5.30. IR (KBr, ν/cm^{-1}): 3049, 2916 ν(C–H), 1641 ν(C = N), 757 ν(C–H) (phenyl).

2.2.2. $[Ni(L_2)_2] \cdot 2(CH_3OH)$ (2). This compound was prepared by the same procedure as described above except that 5-fluorosalicylaldehyde was used instead of 5-chlorosalicylaldehyde. Yield: 0.383 g (78%). IR (KBr, ν/cm^{-1}): 3049, 2916 ν(C–H), 1145 ν(C–F), 1641 ν(C = N), 757 ν(C–H) (phenyl).

2.3. *Physical measurements*

IR spectra were measured using KBr discs on a Vector 22 FT−IR spectrophotometer. UV-Vis spectra were recorded on a UV-2450 spectrophotometer. Circular dichroic spectra of DNA were obtained by using a Jasco J-810 spectropolarimeter.

2.4. *X-ray data collection and refinement*

Crystals were measured on a Bruker AXS SMART diffractometer (Mo-Kα radiation monochromator). The structures were solved by direct methods and refined by full-matrix least-squares on F^2. Hydrogens were located geometrically and refined in riding mode. The non-H atoms were refined with anisotropic displacement parameters. Calculations were performed using SHELX-97 crystallographic software. The crystallographic data and details about the data collection are presented in table 1.

Table 1. Crystal data and structure refinement for the complexes.

	1	2
Empirical formula	$C_{20}H_{26}Cl_2N_2NiO_6$	$C_{20}H_{26}F_2N_2NiO_6$
Formula weight	520.04	487.14
Temperature (K)	291(2)	291(2)
Crystal system	Orthorhombic	Orthorhombic
Space group	*P*212121	*Pna*21
Unit cell dimensions (Å, °)		
a	9.8422(10)	10.3398(13)
b	12.7412(13)	20.631(3)
c	18.1814(19)	9.9464(12)
α	90	90
β	90	90
γ	90	90
Volume (Å^3), *Z*	2280.0(4), 4	2121.75, 4
Calculated density (g cm^{-3})	1.515	1.525
Absorption coefficient μ (Mo-Kα) (mm^{-1})	1.124	0.972
F(000)	1080	1016
Crystal size (mm^3)	0.22 × 0.24 × 0.28	0.22 × 0.24 × 0.28
Mo-Kα radiation (Å)	0.71073	0.71073
θ range for data collection (°)	2.5–26.0	2.0–26.0
*N*ref, *N*par	4462, 282	3876, 282
Total, unique data, *R*(int)	13090, 4462, 0.027	11831, 3876, 0.023
Observed data [$I > 2\sigma(I)$]	4238	3560
W^{-1}	$[S^2(F_o^2) + (0.05P)^2 + 1.99P]$	$[S^2(F_o^2) + (0.03P)^2 + 1.99P]$
P	$P(F_o^2 + 2F_c^2)/3$	$P = (F_o^2 + 2F_c^2)/3$
R, wR_2, *S*	0.0353, 0.1034, 1.07	0.0247, 0.0631, 1.064
Max. and av. shift/error	0.00, 0.00	0.00, 0.00
Resd. dens. (e Å^3)	−0.45 and 0.71	−0.23 and 0.30

2.5. *DNA cleavage experiment*

The cleavage of pBR322 DNA by the complexes was examined by gel electrophoresis. Negative supercoiled pBR322 DNA (0.5 μg μL^{-1}) was treated with different concentrations of the complex (1 μL) in Tris-HCl buffer (1 μL, 50 mmol L^{-1} Tris-HCl, 50 mmol L^{-1} NaCl, pH = 7.2). After mixing, the DNA solutions were incubated at 37°C for 3 h. The reactions were quenched by the addition of sterile solution (1 μL, 0.25% bromophenol blue and 40% w/v sucrose). The samples were then analyzed by electrophoresis for 45 min at 116 V on agarose gel in TAE buffer (2.42 g Tris, 0.57 mL acetic acid, and 0.372 g EDTA in 500 mL doubly distilled water, pH = 7.4, adjusted with HCl). The gel was stained with ethidium bromide (EB, 1 μg μL^{-1}) for 10 min after electrophoresis and then photographed.

3. Results and discussion

3.1. *Structure description*

Perspective views of $[Ni(L_1)_2] \cdot 2(CH_3OH)$ (**1**) and $[Ni(L_2)_2] \cdot 2(CH_3OH)$ (**2**) are given in figure 1(a) and figure 1(b), with the atom numbering schemes. Selected bond lengths and angles relevant to the nickel(II) coordination polyhedron are listed in table 2. Compound **1** contains one Ni(II), two deprotonated ligands, and two methanols.

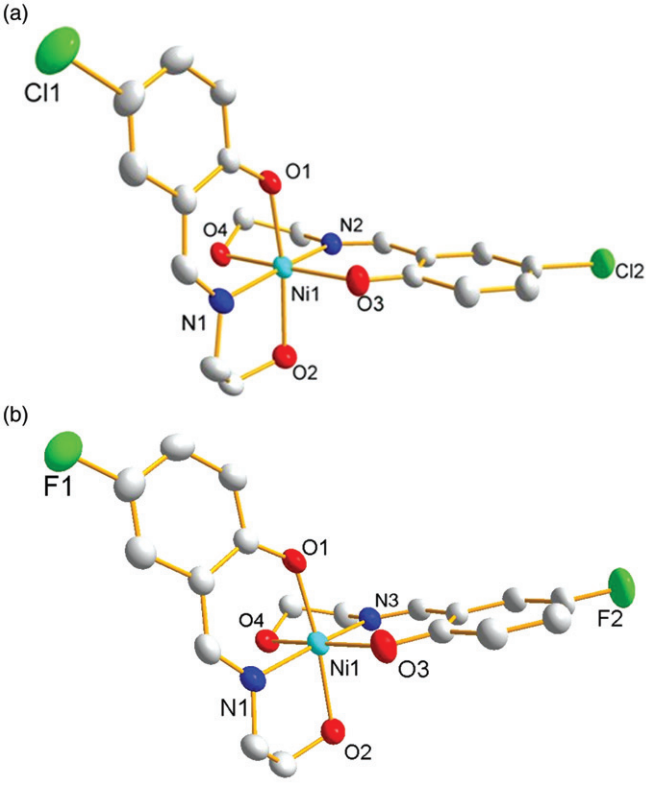

Figure 1. (a) Perspective view of $[Ni(L_1)_2]$. (b) Perspective view of $[Ni(L_2)_2]$.

The coordination polyhedron of Ni(II) can be described as a distorted octahedron. The basal plane is composed of an imine, a phenolate, and a hydroxyl from one ligand and an imine from another ligand. Apical positions are occupied by a phenolate and a hydroxyl from one ligand. The distances between Ni and coordination atoms are in the range 1.997–2.173 Å. Except for carbon connected with hydroxyl, the other atoms in each ligand are almost located in the same plane with mean plane deviation of 0.2841°. The two ligand planes are almost vertical with dihedral angle of 94.9821°.

As shown in figure 2(a), hydrogen-bonding interactions play an important role in maintaining the 2-D network for **1**. Each molecular unit is connected through hydrogen-bonding interactions, including C–H···O and O–H···O. The selected hydrogen-bonding parameters are as follows: $d_{H2\cdots O2} = 2.5500$ Å, $d_{H4A\cdots O1} = 1.9900$ Å and ∠O4–H4A···O1 = 127.00°, ∠C2–H2···O2 = 165.00°.

The structure of **2** is similar to that of **1** with the same coordination polyhedron and donors. There are also abundant hydrogen-bonding interactions in **2** (figure 2b) and relative parameters are as follows: $d_{H8A\cdots F1} = 2.4200$ Å, $d_{H4A\cdots O1} = 1.9700$ Å and ∠O4–H4A···O1 = 137.00°, ∠C8–H8A···F1 = 174.00°. The only difference in molecular composition in **1** and **2** is that the complexes have different substituent on phenolate, R = Cl for **1** and F for **2**, contributing to small differences in relative bond lengths and angles.

Table 2. Selected bond lengths (Å) and angles (°) for the complexes.

Complex **1**		Complex **2**	
Ni1–N1	2.012	Ni1–N1	1.997
Ni1–N3	2.014	Ni1–N3	2.002
Ni1–O1	2.021	Ni1–O1	2.023
Ni1–O2	2.163	Ni1–O2	2.173
Ni1–O3	2.008	Ni1–O3	1.998
Ni1–O4	2.151	Ni1–O4	2.169
O1–Ni1–O3	93.19(9)	O1–Ni1–O3	93.47(6)
O1–Ni1–O2	171.10(10)	O1–Ni1–O2	172.84(6)
O1–Ni1–O4	90.30(9)	O1–Ni1–O4	89.52(6)
O1–Ni1–N1	90.70(10)	O1–Ni1–N1	91.87(7)
O1–Ni1–N2	94.75(10)	O1–Ni1–N3	92.72(6)
O2–Ni1–O3	89.54(10)	O2–Ni1–O3	88.86(6)
O2–Ni1–O4	88.25(9)	O2–Ni1–O4	89.03(6)
O2–Ni1–N1	80.62(11)	O2–Ni1–N1	81.19(7)
O2–Ni1–N2	93.70(11)	O2–Ni1–N3	93.99(6)
O3–Ni1–N2	90.39(11)	O3–Ni1–N3	91.67(7)
O3–Ni1–N1	94.97(11)	O3–Ni1–N1	94.27(7)
O3–Ni1–O4	171.04(10)	O3–Ni1–O4	172.24(6)
N1–Ni1–N2	172.14(12)	O4–Ni1–N3	81.03(6)
O4–Ni1–N1	93.24(10)	O4–Ni1–N1	92.79(7)
O4–Ni1–N1	93.24(10)	N1–Ni1–N3	172.27(8)

3.2. *Absorption spectroscopic studies*

Electronic absorption spectroscopy is employed to determine the binding characteristics of metal complexes with DNA. Absorption spectra of **1** and **2** in the absence and presence of CT-DNA at different concentrations (0–75 μmol L^{-1}) are shown in figure 3(a) and figure 4(a); there is not much difference for these two complexes.

In the UV region, with increasing CT-DNA concentration for **1**, hypochromism in the band at 383 nm reaches as high as 53% with a red shift of 5 nm. The band at 383 nm in **2** shows hypochromism by 49% and a red shift of 5.85 nm under the same experimental conditions.

In order to quantitatively investigate the binding strength of the complex with CT-DNA, the intrinsic binding constant K_b was obtained by monitoring the changes in absorbance at 380 nm for the complex with increasing concentration of CT-DNA using the equation $[DNA]/E_{ap} = [DNA]/E + 1/(K_bE)$, where $E_{ap} = \epsilon_a - \epsilon_f$, $E = \epsilon_b - \epsilon_f$; ϵ_a, ϵ_f, and ϵ_b correspond to $A_{obs}/[L]$, the extinction coefficients for the free complex and the complex in the fully bound form, respectively, and through the ratio of slope to the intercept from the plots of $[DNA]/E_{ap}$ *versus* [DNA] [9]. As shown in figures 3(b) and 4(b), the calculated K_b values were $0.85 \times 10^5 (\text{mol L}^{-1})^{-1}$ for **1** and $0.88 \times 10^5 (\text{mol L}^{-1})^{-1}$ for **2**, which fit values of classical intercalation. The large hypochromity and the red shift illustrate that the interaction between CT-DNA and the complexes is intercalative, indicating that the complexes interact with DNA through a stacking interaction between the aromatic chromophore in the complexes and the base pairs of DNA [1–13].

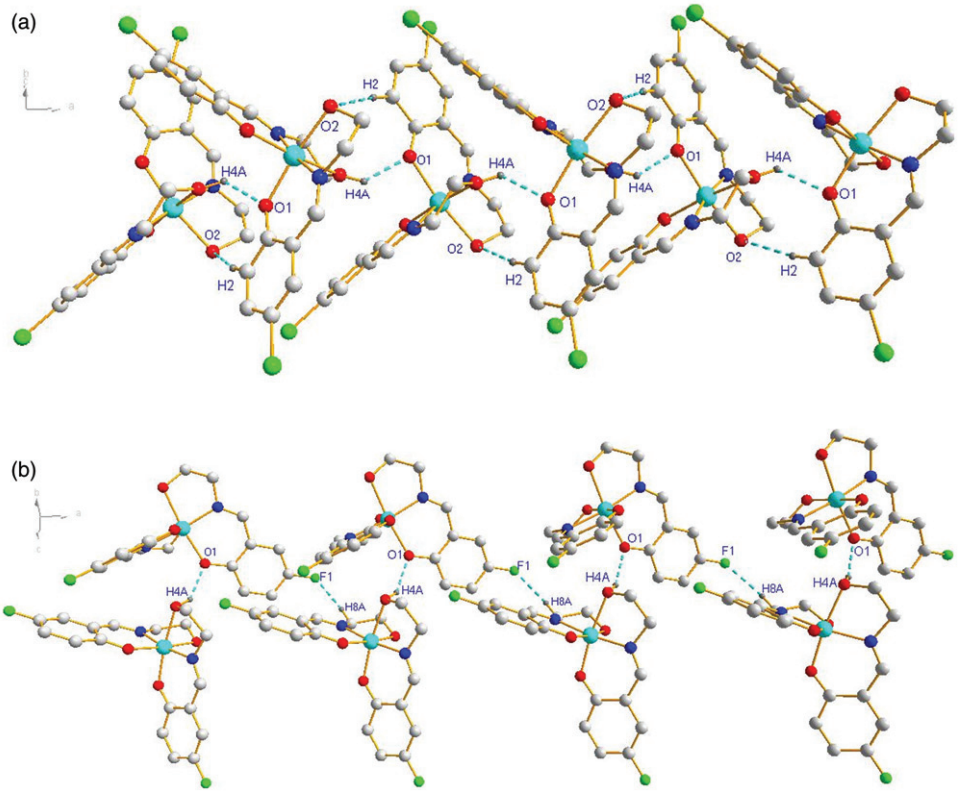

Figure 2. (a) View of the 2-D network of **1** depicting the connection *via* C–H···O and O–H···O hydrogen bonds; dashed lines indicate hydrogen bonds. (b) View of the 2-D network of **2** depicting the connection *via* C–H···O and O–H···F hydrogen bonds; dashed lines indicate hydrogen bonds.

3.3. *Interaction between the complex and plasmid DNA(pBR 322)*

DNA cleavage experiments were performed using a double-stranded DNA plasmid. The metal complexes cause random nicks (cuts) to one of the DNA strands. As a consequence, the supercoiled form opens to an open circular form after one nick and subsequently to a linear form (linear DNA) if two nicks on complementary strands are within a short distance.

Finally, the DNA gets degraded into small pieces of different size which cannot be detected in our assay. The cleavage products were subjected to gel electrophoretic separation and the gels were analyzed after EB staining.

The DNA cleaving ability was investigated with various concentrations and incubation time intervals (figures 5 and 6). From figure 5, we know that the cleavage activity of **1** increased with incubation time, while **2** exhibited a cleavage activity independent of incubation time. On the other hand, the concentration of the complex has little effect on the cleavage activity of **1** in the range 12.5–200 μmol L^{-1}, but cleavage activity of **2** increases with increase in concentration. The obvious DNA cleaving activity of the complexes at lower concentration of 12.5 μmol L^{-1} indicates strong interactions with DNA, which are in agreement with the spectroscopic results.

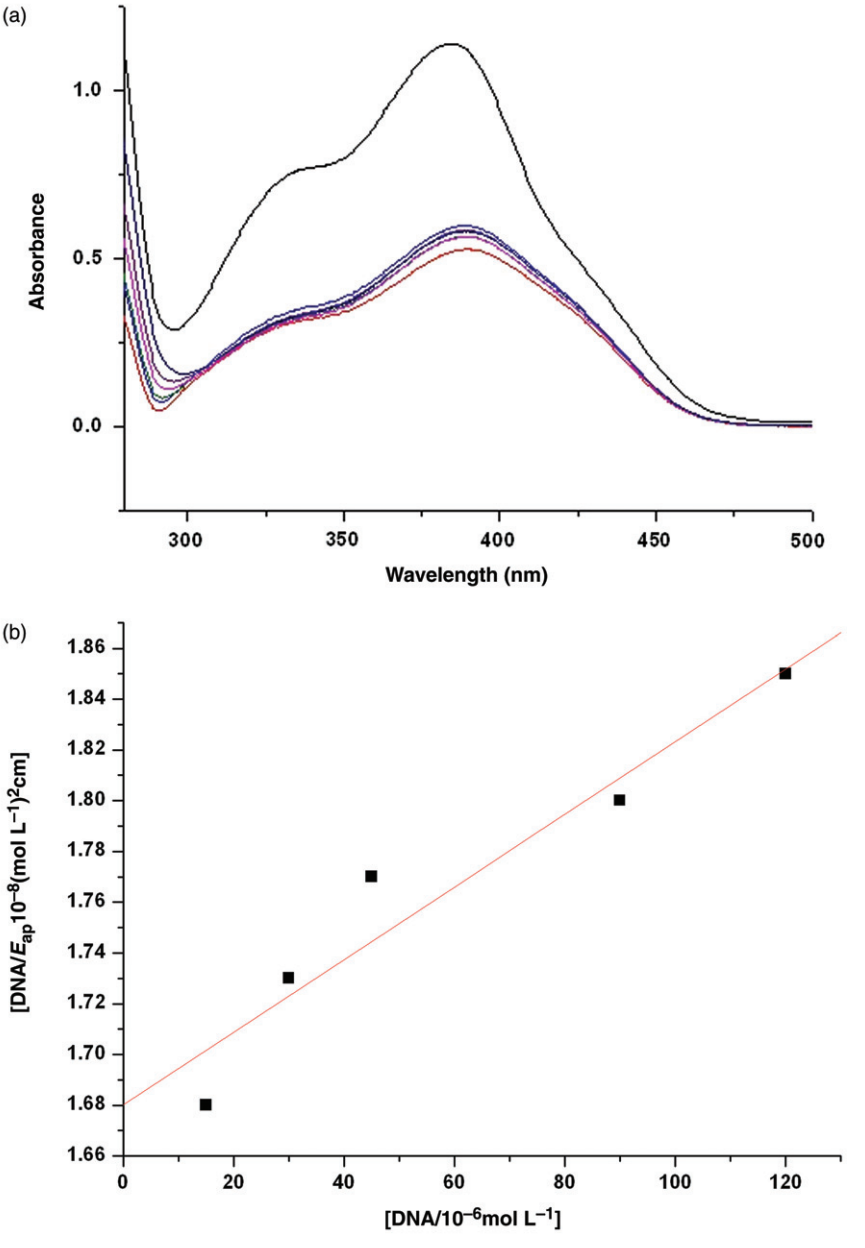

Figure 3. (a) Absorption spectra of **1** in Tris-HCl buffer upon addition of CT-DNA. (b) Plot of [DNA]/E_{ap} *vs.* [DNA] for absorption titration of CT-DNA with **1**.

To examine the DNA cleavage mechanism by the complexes scavenging agents, hydroxyl radical scavengers (5 mmol L^{-1} DMSO), superoxide scavenger (5 mmol L^{-1} KI), and singlet oxygen scavenger (5 mmol L^{-1} NaN_3) were added in the incubation solution. The results of DNA cleavage in the presence or absence of the scavenging agents by the complexes are presented in figure 7. Addition of scavenging agents has

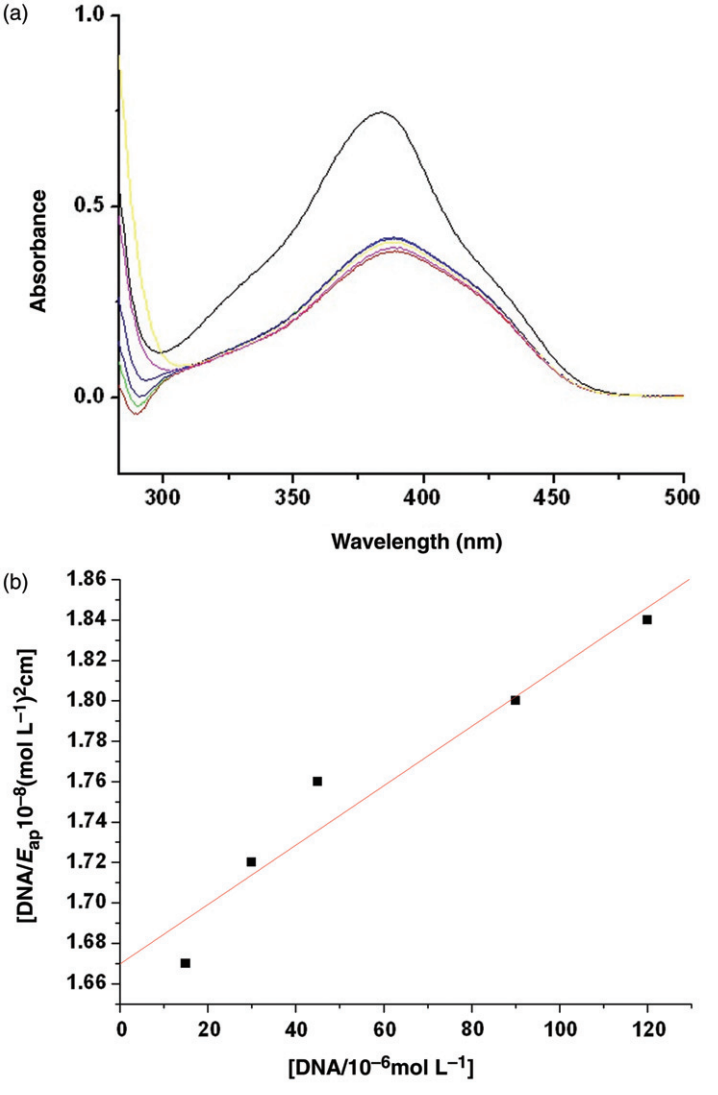

Figure 4. (a) Absorption spectra of **2** in Tris-HCl buffer upon addition of CT-DNA. (b) Plot of [DNA]/E_{ap} *vs.* [DNA] for absorption titration of CT-DNA with **2**.

little effect on DNA cleavage, indicating that oxidative cleavage is not responsible for the cleavage activity. Therefore, the DNA cleavage activity by **1** and **2** is ascribed to hydrolytic cleavage.

4. Conclusions

Reactions between 5-X-salicylaldehyde (X = F and Cl) and 2-aminoethanol in the presence of nickel(II) yield two new mononuclear nickel(II) complexes. The crystal

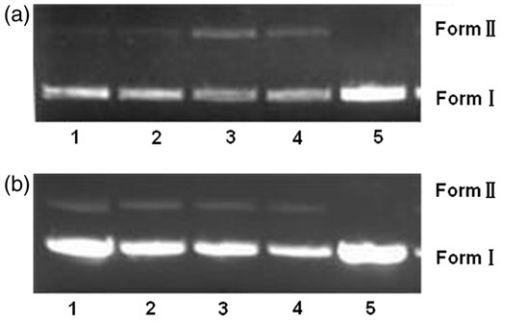

Figure 5. Gel electrophoresis diagram showing the cleavage of pBR322 DNA ($0.5\,\mu g\,\mu L^{-1}$) by the complexes ($50\,\mu mol\,L^{-1}$) in $50\,mmol\,L^{-1}$ Tris-HCl/NaCl buffer (pH 7.2) and 37°C for different incubation time: Lanes 1–4, DNA + complex ($50\,\mu mol\,L^{-1}$) for 1 h, 2 h, 3 h, 4 h; Lane 5, DNA control; a for **1** and b for **2**.

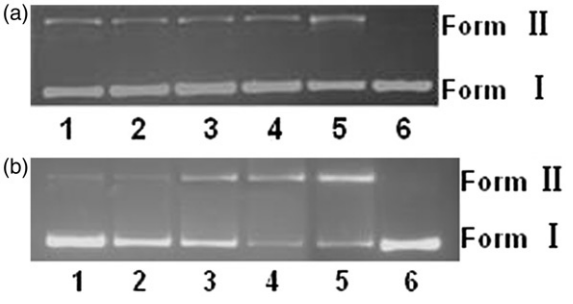

Figure 6. Gel electrophoresis diagram showing the cleavage of pBR322 DNA ($0.5\,\mu g\,\mu L^{-1}$) by the complexes at different concentrations in $50\,mmol\,L^{-1}$ Tris-HCl/NaCl buffer (pH 7.2) and 37°C for 3 h: Lanes 1–5, DNA + complex ($12.5\,\mu mol\,L^{-1}$, $25\,\mu mol\,L^{-1}$, $50\,\mu mol\,L^{-1}$, $100\,\mu mol\,L^{-1}$, and $200\,\mu mol\,L^{-1}$), respectively; Lane 6, DNA control; a for **1** and b for **2**.

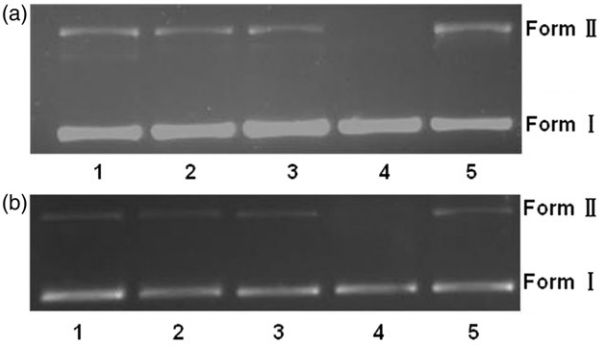

Figure 7. Gel electrophoresis diagram showing the cleavage of pBR322 DNA ($0.25\,\mu g\,\mu L^{-1}$) by the complexes with different scavenging agents in $50\,mmol\,L^{-1}$ Tris-HCl/NaCl buffer (pH 7.2) and 37°C for 3 h: Lanes 1–3, DNA + complex ($12.5\,\mu mol\,L^{-1}$) + $5\,mmol\,L^{-1}$ NaN_3; KI; DMSO; Lane 4, DNA control; Lane 5, DNA + complex ($12.5\,\mu mol\,L^{-1}$); a for **1** and b for **2**.

packing of the complexes reveal abundant hydrogen-bond interactions. UV-Vis spectra and agarose gel electrophoresis show that the nickel(II) complexes of 4-X-2-((2-hydroxyethylimino)methyl)phenol have strong interactions with DNA in an intercalative mode, and the complexes exhibit effective DNA cleavage activity even in a lower concentration through a hydrolytic cleavage mechanism. However, the corresponding binding constants are smaller because of the flexibility of the ligand, showing the importance of ligand on the binding constant. As the planarity of the intercalating ligand increases, binding constant increases and asymmetry of the ligand makes it difficult to intercalate, and hence the binding constant decreases [14, 15].

Acknowledgments

We are grateful for the financial support from the National Nature Science Foundation of China (20971102, 20871097) and the Foundation of the Excellent Middle-Young Innovation Group of Education Department of Hubei province (T200802), China.

References

[1] J.E. Deweese, F.P. Guengerich, A.B. Burgin. *Biochemistry*, **48**, 38 (2009).
[2] N. Raman, J. Dhaveethu Raja. *J. Chem. Sci.*, **119**, 4 (2007).
[3] G. Fei, Y. Caixia, Y. Pin. *Chin. Sci. Bull.*, **49**, 16 (2004).
[4] S.I. Kirin, C.M. Happel, S. Hrubanova, T. Weyhermuller. *Dalton Trans.*, 1201 (2004).
[5] C.L. Liu, S. Yu, D.F. Li, Z. Liao. *Inorg. Chem.*, **41**, 4 (2002).
[6] S. Thakurta, P. Roy, G. Rosair. *Polyhedron*, **28**, 695 (2009).
[7] R.L. De, K. Samanta, K. Maiti. *Inorg. Chim. Acta*, **316**, 3 (2001).
[8] Y.M. Chumakova, V.I. Tsapkov. *J. Mol. Struct.*, **647**, 3 (2003).
[9] A.M. Pyle, J.P. Rehmann, C.V. Kumar. *J. Am. Chem. Soc.*, **111**, 3051 (1989).
[10] J. Liu, T.B. Lu, H. Li. *Transition Met. Chem.*, **27**, 686 (2002).
[11] P. Uma Maheswari, M. Palaniandavar. *J. Inorg. Biochem.*, **98**, 219 (2004).
[12] S. Wu, Z. Li, L. Ren, B. Chen, F. Liang, X. Zhou, T. Jia, X. Cao. *Bioorg. Med. Chem.*, **14**, 2956 (2006).
[13] J.L. Tian, L. Feng, W. Gu, G.J. Xu, S.P. Yan, D.Z. Liao, Z.H. Jiang, P. Cheng. *J. Inorg. Biochem.*, **101**, 196 (2007).
[14] C. Gao, X.F. Ma, J. Tian, D.D. Li. *J. Coord. Chem.*, **63**, 115 (2010).
[15] K. Laxma Reddy, K. Ashwini Kumar, S. Vidhisha. *J. Coord. Chem.*, **62**, 3997 (2009).